VIROLOGY 249, 379–392 (1998)
ARTICLE NO. VY989341

In Vitro Characterization of Late Steps of RNA Recombination in Turnip Crinkle Virus

I. Role of the Motif1-Hairpin Structure

Peter D. Nagy and Anne E. Simon[1]

Department of Biochemistry and Molecular Biology, Program in Molecular and Cellular Biology, University of Massachusetts, Amherst, Massachusetts 01003

Received May 11, 1998; returned to author for revision June 16, 1998; accepted July 22, 1998

Molecular mechanisms of RNA recombination were studied in turnip crinkle carmovirus (TCV), which has a uniquely high recombination frequency and nonrandom crossover site distribution among the recombining TCV-associated satellite RNAs. An *in vitro* system has been developed that includes a partially purified TCV replicase preparation (RdRp) and chimeric RNAs that resemble the putative *in vivo* recombination intermediates (Nagy, P. D., Zhang, C., and Simon, A. E. *EMBO J.* 17, 2392–2403, 1998). This system generates 3′-terminal extension products, which are analogous to the recombination end products. Efficient generation of 3′-terminal extension products depends on the presence of a hairpin structure (termed the motif1-hairpin) that possibly binds to the RdRp. Replacement of the motif1-hairpin with two separate randomized sequences resulted in a basal level of 3′-terminal extension. By using three separate constructs, each carrying similar mutations in the motif1-hairpin, we demonstrate that the role of the motif1-hairpin in 3′-terminal extension is complex and its function is influenced by flanking sequences. In addition to the mutagenesis approach, competition experiments between wild-type and mutated motif1-hairpin constructs suggest that the TCV RdRp likely recognizes the secondary and/or tertiary structure of the motif1-hairpin, while individual nucleotides play a less important role. Overall, the data shed new light into the mechanism of 3′-terminal extension by a viral RdRp that is analogous to the late steps of RNA recombination in TCV.

Key Words: plant virus; recombination; replication; satellite RNA; template switching.

INTRODUCTION

Genetic RNA recombination, a process that joins together two noncontiguous RNA segments, is well documented for a large number of animal and plant viruses and bacteriophages (King, 1988; Lai, 1992; Simon and Bujarski, 1994). RNA recombination can create novel chimeric viruses and functional genomes from mutated (damaged) RNAs and may also contribute to the quasispecies nature of RNA viruses (Zimmern, 1988; Lai, 1992; White and Morris, 1995; Nagy and Bujarski, 1996; Simon and Nagy, 1996). Due to these characteristics, RNA recombination is believed to be a major force in viral evolution and adaptation (Strauss and Strauss, 1988; King, 1988; Lai, 1992; Dolja and Carrington, 1992; Simon and Bujarski, 1994).

Mechanistic studies on RNA recombination favor replicase (RNA-dependent RNA polymerase, RdRp)-driven template switching models (King, 1988; Jarvis and Kirkegaard, 1991; Lai, 1992; Nagy and Simon, 1997), although RNA breakage and religation may also occur *in vitro* (Chetverin *et al.,* 1997). Based on the putative structure of recombination intermediates, the recombination end products, and components of the recombination machinery, RNA recombination can be divided into three major classes: (1) similarity essential; (2) similarity nonessential, and (3) similarity assisted (Nagy and Simon, 1997). Similarity-essential recombination events require substantial sequence similarity between the parental RNAs, which is the major RNA determinant in selection of recombination junction sites. The recombination end products are either precise or imprecise. Similarity-nonessential recombination does not require sequence similarity between the parental RNAs. Rather, similarity-nonessential recombination events are driven by various features of the RNA templates, such as heteroduplex formation between the parental RNAs, RdRp-binding sequences, and/or secondary structure elements. Similarity-assisted recombination events require sequence similarity between the parental templates. However, unlike similarity-essential recombination, additional RNA determinants, such as an RdRp-binding sequence present in one of the RNAs, are essential for this type of recombination event (Nagy and Simon, 1997). Among the best characterized RNA recombination systems, similarity-essential and similarity-nonessential RNA recombination have been proposed to occur in brome mosaic virus (BMV, Nagy and Bujarski, 1993, 1995, 1997), while similarity-assisted RNA recombination has been characterized in turnip crinkle virus (TCV, Simon and Nagy, 1996; Nagy *et al.,* 1998).

Due to the complex nature of RNA recombination events, it is important to analyze the role of the RNA and

[1] To whom reprint requests should be addressed.

0042-6822/98 $25.00

protein components of the recombination machinery separately. Based on the replicase-mediated template-switching model, recombination events are divided into two groups: (1) early steps that include the donor RNA as a template and lead to the synthesis of the nascent primer strand from the donor RNA and (2) late steps that include the acceptor RNA as template. In mechanistic terms, the late steps include the transfer of the nascent primer strand and binding of the RdRp to the acceptor RNA followed by primer elongation on the acceptor RNA (Nagy and Simon, 1997; Nagy *et al.,* 1998). To test these steps separately, we have developed an *in vitro* system in TCV that does not require the amplification of recombination products (Nagy *et al.,* 1998).

TCV is a 4054-base RNA virus that is uniquely associated with a number of subviral RNAs, including satellite (sat-RNA D, 194 nt) and chimeric RNAs (sat-RNA C, 356 nt) (Simon and Nagy, 1996). Sat-RNA C, which is composed of sequences similar to sat-RNA D at its 5′ end and two 3′ proximal regions from TCV genomic RNA at its 3′ end, is the product of natural recombination (Simon and Howell, 1986). High-frequency recombination was observed *in vivo* between sat-RNA D and sat-RNA C with the recombination junctions clustered near the 3′ end of sat-RNA D and at the base of a hairpin (designated motif1-hairpin) in the central portion of sat-RNA C (Cascone *et al.,* 1990, 1993). Noncompensatory mutations in the stem of the motif1-hairpin eliminated detectable recombinants *in vivo* (Cascone *et al.,* 1990, 1993; Nagy *et al.,* 1998). Based on these and other observations, a template-switching model was proposed in which the viral RdRp uses the nascent, positive-stranded sat-RNA D as a primer to resume RNA elongation on the acceptor minus-stranded sat-RNA C template (Cascone *et al.,* 1993; Simon and Nagy, 1996; Fig. 1A). The model proposed that the motif1-hairpin is involved in recruitment of the RdRp during reinitiation of synthesis following the template switch.

An *in vitro* system has been developed to mimic this *in vivo* recombination event (Nagy *et al.,* 1998). The template for the *in vitro* system is a chimeric RNA containing the *in vivo* hot-spot region from sat-RNA D plus strands at the 3′ end joined to the hot-spot region from sat-RNA C minus strands including the motif1-hairpin (Fig. 1B). Partially purified TCV RdRp generated hairpin-like products by intramolecular extensions from the 3′ end of the chimeric template (Nagy *et al.,* 1998). This study revealed roles for two separate sequences on the acceptor sat-RNA C-derived region in 3′-terminal extension. One sequence 3′ of the motif1-hairpin served to bind the plus-stranded sat-RNA D sequence (called the priming stem). The other sequence, motif1-hairpin, is the primary candidate for specific recognition by the TCV RdRp (Nagy *et al.,* 1998, Fig. 1). The putative role of the motif1-hairpin in RdRp binding was supported by competition experiments in which sequences containing the wt motif1-hairpin competed more efficiently with 3′-terminal extension activity from a template RNA than sequences with motif1-hairpin mutations or heterologous tRNA (Nagy *et al.,* 1998). Mutations that destabilized the motif1-hairpin were the best inhibitors of 3′-terminal extension, suggesting a role for the motif1-hairpin structure in 3′-terminal extension. In addition, specific mutations within the bulge and loop regions in the motif1-hairpin decreased 3′-terminal extension to a low level, indicating that these sequences may be involved specifically in RdRp binding (Nagy *et al.,* 1998). The same regions were also important in *in vivo* RNA–RNA recombination between sat-RNA C and sat-RNA D (Cascone *et al*. 1993; Nagy *et al.,* 1998). Overall, these studies demonstrated that the *in vitro* 3′-terminal extension reaction mimics the late steps of *in vivo* RNA recombination: strand transfer and primer elongation.

In this report, we extend the analysis of the role of the motif1-hairpin in 3′-terminal extension reaction and in putative RdRp binding. Extensive mutagenesis of the motif1-hairpin was conducted, and the effect of mutations on 3′-terminal extension was tested in three separate constructs. These constructs contained different flanking sequences, and their use in combination with competition experiments between wt and mutant motif1-hairpin containing constructs allowed for discrimination between direct and indirect effects of the mutations on RdRp binding and 3′-terminal extension reactions. The results support both direct and indirect roles for the motif1-hairpin in 3′-terminal extension. The data are consistent with a secondary/tertiary structure-based recognition of the motif1-hairpin by the TCV RdRp, while the primary sequence of the hairpin plays a less important role. We propose that the recognition of the motif1-hairpin by the TCV RdRp is similar to the RdRp's recognition of the negative strand initiation promoter and the subgenomic promoter.

RESULTS AND DISCUSSION

Basal level of 3′-terminal extension activity in the absence of the motif1-hairpin

Specific interactions between viral RNAs and viral RdRps are fundamental in RNA replication and recombination (Buck, 1996; Lai, 1992; Nagy and Simon, 1997). The complex nature of the interaction in viral RNA replication systems, however, makes it difficult to address the basic question of what RNA features are recognized by the RdRp and used to discriminate against other potential binding sites. Much more progress has been achieved with simpler systems, such as tRNA interaction with aminoacyl-tRNA synthetases and recognition of the HIV TAR and RRE elements by Tat and Rev proteins (Draper, 1995). These and other studies revealed that proteins can recognize various features in RNAs, including single-stranded regions, hairpins, bulges, loops, pseudoknots, irregular helices, and tertiary structures stabilized by bound cations.

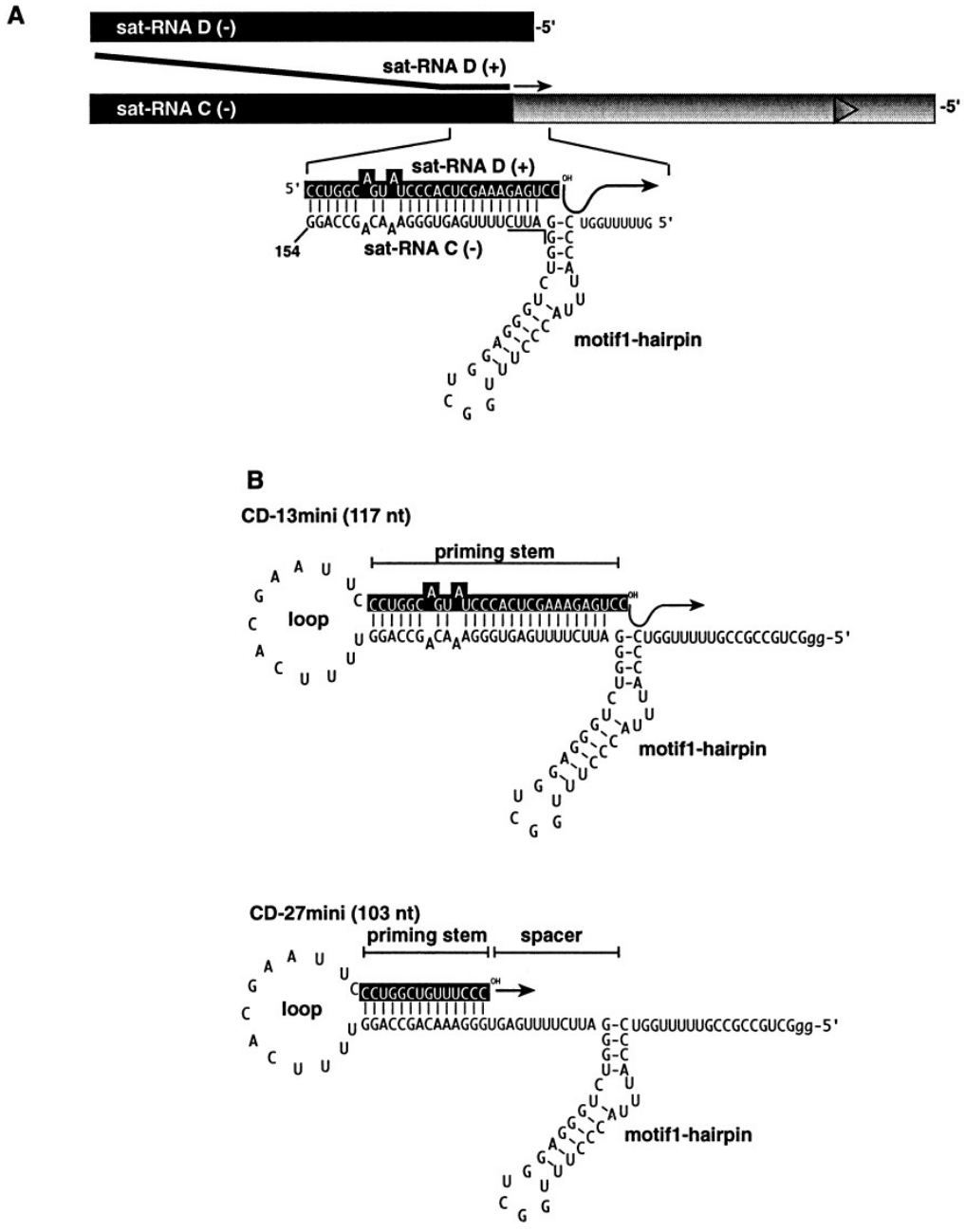

FIG. 1 An *in vitro* system to study the late steps of RNA recombination in TCV. (A) Model for *in vivo* RNA recombination between sat-RNA D and sat-RNA C by a replicase-driven template switching mechanism. The recombination intermediates are depicted showing the possible RNA–RNA interaction between the nascent sat-RNA D plus-strand, truncated at position −13 at the 3′ end (in *in vivo* experiments, the junctions were located most frequently at positions −13 to −15, as counted from the 3′ end), and sequence 3′ of the motif1-hairpin of minus-strand sat-RNA C (the acceptor RNA strand). Sat-RNA D sequence is boxed in black. Underlined nts at the base of the motif1-hairpin indicate the location of the *in vivo* junction site hot-spot in sat-RNA C. In the rectangles representing the sat-RNAs, similar regions are shaded alike. A triangle represents a positive-strand initiation promoter (Guan *et al.,* 1997). (B) *In vitro* system that mimics the putative *in vivo* recombination intermediate. Top construct (CD-13mini) contains 28 nts from sat-RNA D plus strand (boxed in black), extending from position −13 at the 3′ end, joined by a 6-base artificial sequence (GAAUUC) to sat-RNA C minus-strand sequence that includes 33 nt 3′ of the motif1-hairpin, the motif1-hairpin, and 18 nts 5′ of the hairpin with two nonviral G residues at the 5′ end (shown by lower case letters). Bottom construct (CD-27mini), same as CD-13mini, except that the sat-RNA D sequence terminates at the −27 position and two mismatches in the priming stem are mutated such that base-pairing can occur throughout the priming stem. Regions referred to in the text as the priming stem, motif1-hairpin, loop, and spacer are shown.

Mutagenesis approaches have been used to make low-resolution maps for many RNA–protein complexes (Draper, 1995). Deletion or mutation of a particular nucleotide can affect protein binding directly at the contact sites or indirectly by affecting the folding of the RNA. The folding of the RNA can be important prior to and/or after protein binding, which usually induces substantial conformational changes in the RNA structure. Since cur-

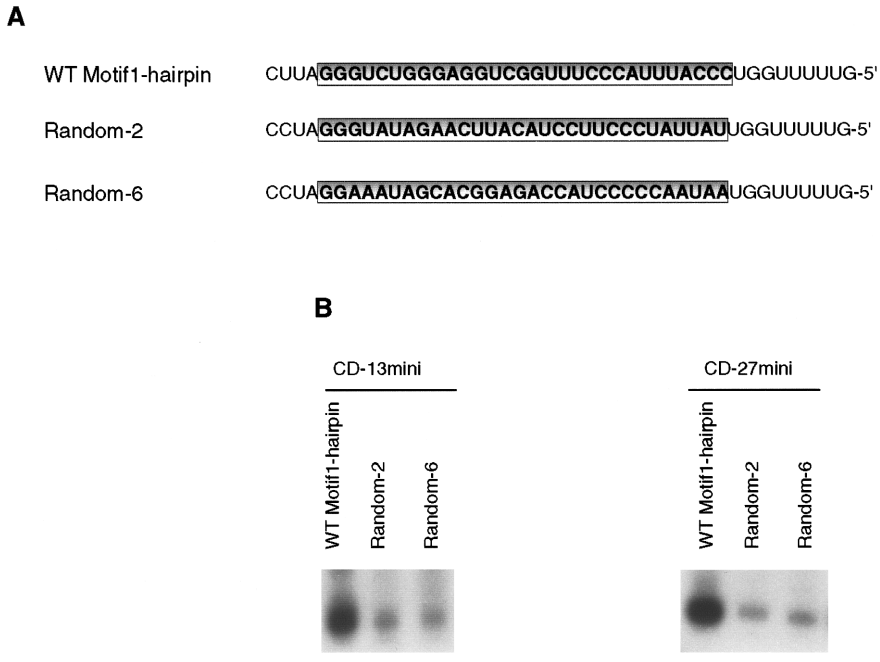

FIG. 2. (A) Sequence of the wt motif1-hairpin and two heterologous sequences, termed random2 and random6, which were used to replace the motif1-hairpin in CD-13mini and CD-27mini (Fig1B). (B) Representative experiment showing denaturing gel analysis of radiolabeled 3′-terminal extension products synthesized by *in vitro* transcription with TCV RdRp using either CD-13mini (left) or CD-27mini (right).

rently it is not possible to predict what kinds of RNA features are recognized by viral RdRps, detailed studies will be needed to unravel RNA–protein interactions in replication and recombination of RNA viruses.

We have recently developed an *in vitro* system that mimics RNA recombination between sat-RNA C and sat-RNA D, including the strand transfer and primer elongation steps (Nagy *et al.,* 1998). This system utilizes partially purified, template-dependent TCV RdRp preparations (Song and Simon, 1994) programmed with a chimeric RNA template (construct CD-13mini, Fig. 1B) designed to resemble *in vivo* recombination intermediates (Nagy *et al.,* 1998). CD-13mini consisted of sequences corresponding to the central portions of the negative strand of sat-RNA C (including the *in vivo* recombination hot-spot region and the motif1-hairpin) and a 28-nt segment of positive-strand sat-RNA D with the 3′ terminus representing the *in vivo* recombination hot-spot (position −13 relative to the 3′ end). A 6-nt artificial loop sequence was used to covalently link the sat-RNA D plus-strand fragment to the sat-RNA C minus-strand fragment, as depicted in Fig. 1B, to ensure that an optimal 1:1 molar ratio of interacting sequences were in proximity and in the correct orientation. Sequence complementarity between the 3′-end region of sat-RNA D positive-strand and a region 3′ of the motif1-hairpin in the negative-strand of sat-RNA C is predicted to form a stable base-paired structure (the priming stem). The TCV RdRp starts 3′-terminal extension at the "natural" recombination hot-spot region (i.e., at the base of the motif1-hairpin, Fig. 1). This "self-primed" 3′-terminal extension reaction generates a product that has a hairpin-like structure with long double-stranded region and short loop sequence (Nagy *et al.,* 1998). Construct CD-27mini is the same as CD-13mini except that the sat-RNA D sequence terminates at the −27 position and two mismatches in the priming stem are mutated such that base pairing can occur throughout the priming stem (Fig. 1B). CD-27mini, which due to the short priming stem and a flexible spacer between the priming stem and the motif1-hairpin, supports 3′-terminal extension about sixfold more efficiently than CD-13mini (Nagy *et al.,* 1998; data not shown).

To establish the basal level of 3′-terminal extension in the absence of the motif1-hairpin, two 30-nt-long randomized (heterologous) sequences were used to replace the similar-sized motif1-hairpin sequence in CD-13mini and CD-27mini (Fig. 2A). The resulting constructs (random2 and random6) were used to program partially purified TCV RdRp preparations followed by denaturing urea/PAGE analysis of 3′-terminal extension products as described under Materials and Methods. Quantitation of the 3′-terminal extension products by densitometric scanning of exposed films followed by normalization for the number of adenylate residues on the template portion of the respective RNA was used to measure the amount of 3′-terminal extension products in the *in vitro* RdRp assay. Constructs random2 and random6 supported 3′-terminal extension at 3–5% of the wt level in both CD-13mini and CD-27mini (Fig. 2B). Deletion of the 5′- half of the motif1-hairpin also resulted in 3% 3′-terminal extension activity (Nagy *et al.,* 1998), suggesting that the contribution of the motif1-hairpin to the efficiency of 3′-terminal extension is 20- to 30-fold. Overall, these

data demonstrate that the basal level of 3′-terminal extension activity that occurs in the absence of the motif1-hairpin is very low.

Experimental design to study the role of the motif1-hairpin in 3′-terminal extension

To characterize the role of individual bases within the motif1-hairpin in detail, we mutagenized the motif1-hairpin extensively and tested the 3′-terminal extension activity of the resulting constructs in a TCV RdRp assay (Figs. 3 and 5–7; Nagy *et al.,* 1998). The goal of these studies was to find primary sequences and/or secondary structures of the motif1-hairpin that may be important in binding to the TCV RdRp prior to the 3′-terminal extension reaction. The *in vitro* system measures the extent of 3′-terminal extension that can be influenced by motif1-hairpin mutations directly (i.e., altering the efficiency of RdRp binding) or indirectly (e.g., changing the secondary/tertiary structure of the RNA template). To differentiate between direct and indirect effects of mutations, we tested the effect of motif1-hairpin mutations on 3′-terminal extension in three different constructs.

One construct was CD-27mini described above (Fig. 1B). The second construct was CD-14B, which contains the "natural" priming stem that results in initiation of terminal elongation at the recombination hot-spot region (Nagy *et al.,* 1998; see Fig. 3A). The third construct was CD-27, which is similar to CD-14B except that the satRNA-D-derived sequence terminates at position −27 and the priming stem contains no mismatch nucleotides (Fig. 3A). These modifications in CD-27 create a single-stranded spacer between the motif1-hairpin and the priming stem that likely increases the flexibility of the positioning between structured priming-stem and the motif1-hairpin (Fig. 3A). The presence of extensive 5′ sequences in CD-14B and CD-27, which includes a known positive strand initiation promoter (Guan *et al.,* 1997), creates the possibility of interactions between the motif1-hairpin and the 5′ sequences, or the possible competition for RdRp binding between the motif1-hairpin and the 5′ proximal promoter sequences. These factors may inhibit 3′-terminal extension since CD-27 is approximately twofold less active in 3′-terminal extension than CD-27mini, which lacks lengthy 5′ sequences (data not shown).

The use of three sets of constructs should allow for discrimination between direct and indirect effects of motif1-hairpin mutations on 3′-terminal extension based on the following predictions: (1) if the motif1-hairpin mutations were to have similar effects in all three sets of constructs, that would suggest a specific role for the particular sequence/structure in 3′-terminal extension, possibly by altering RdRp binding to the motif1-hairpin. (2) If the CD-27 series was to show similar effects to the CD-14B series but different from the CD-27mini series for a particular mutation, this would suggest that the mutation changed the interactions between the 5′ flanking sequences and the motif1-hairpin. Alternatively, it could indicate that this mutation alters the possible competitiveness of the motif1-hairpin in its capacity to bind to the RdRp when compared to the upstream promoter sequence. (3) If the CD-27 series of mutants behaves like those of the CD-27mini but different from CD-14B, this would support an indirect role for the "positioning" of the motif1-hairpin and the priming stem. (4) If all three series of mutants were to produce different 3′-terminal extension results, then the involvement of multiple features or interactions among these sequences would be likely.

Effect of mutations in the loop region on the efficiency of 3′-terminal extensions

Loop sequences are frequently recognized by proteins (Draper, 1995). Using a single construct (CD-14B), we previously showed that mutations at positions 193 and 196 in the 6-nt-long loop of the motif1-hairpin reduced 3′-terminal extension activity by about fourfold and eliminated *in vivo* recombination (Nagy *et al.,* 1998). This result suggested that the loop region may play a specific role in recombination and possibly in RdRp binding.

To further investigate the role of specific loop nucleotides in 3′-terminal extension, mutations were constructed in all loop positions and tested in CD-14B, CD-27, or CD-27mini. The level of 3′-terminal extension for each motif1-hairpin mutant was compared to the level of 3′-terminal extension obtained with the wt motif1-hairpin present in the corresponding wt construct (i.e., CD-14B, CD-27, and CD-27mini, respectively, representing 100% value in each set). The results of the 3′-terminal extension reactions will be described with the minimum and maximum values for each loop mutant when the particular mutation in the three sets of constructs gave comparable results. We will specify in detail those cases when the three constructs resulted in very different 3′-terminal extension values.

The name of the individual constructs and the introduced mutations are shown in Fig. 3B, while the results of the 3′-terminal extension reaction are shown in Fig. 3C. Constructs G191C, U192A, G194A, G195U, U196C, and U196G with single mismatch mutations within the loop-region generated 3′-terminal extension products at 25.9–47.6% of the level of the wt constructs, while constructs with mutations at position 193 (C193U, C193G, Fig. 3A) had the lowest 3′-terminal extension activity (between 13.1 and 43.6%). Double mutants (constructs U192C/C193G, C193U/U196A, U196G/U197A) produced 3′-terminal extension products at a level similar to the above single mutants (between 14.6 and 49.6% of wt, Fig. 3B). The observation that mutations within the loop region decreased 3′-terminal extension activity more than 50% with all three sets of constructs suggests a specific role for the loop region in 3′-terminal extension. However, none of the loop mutations tested showed a basal

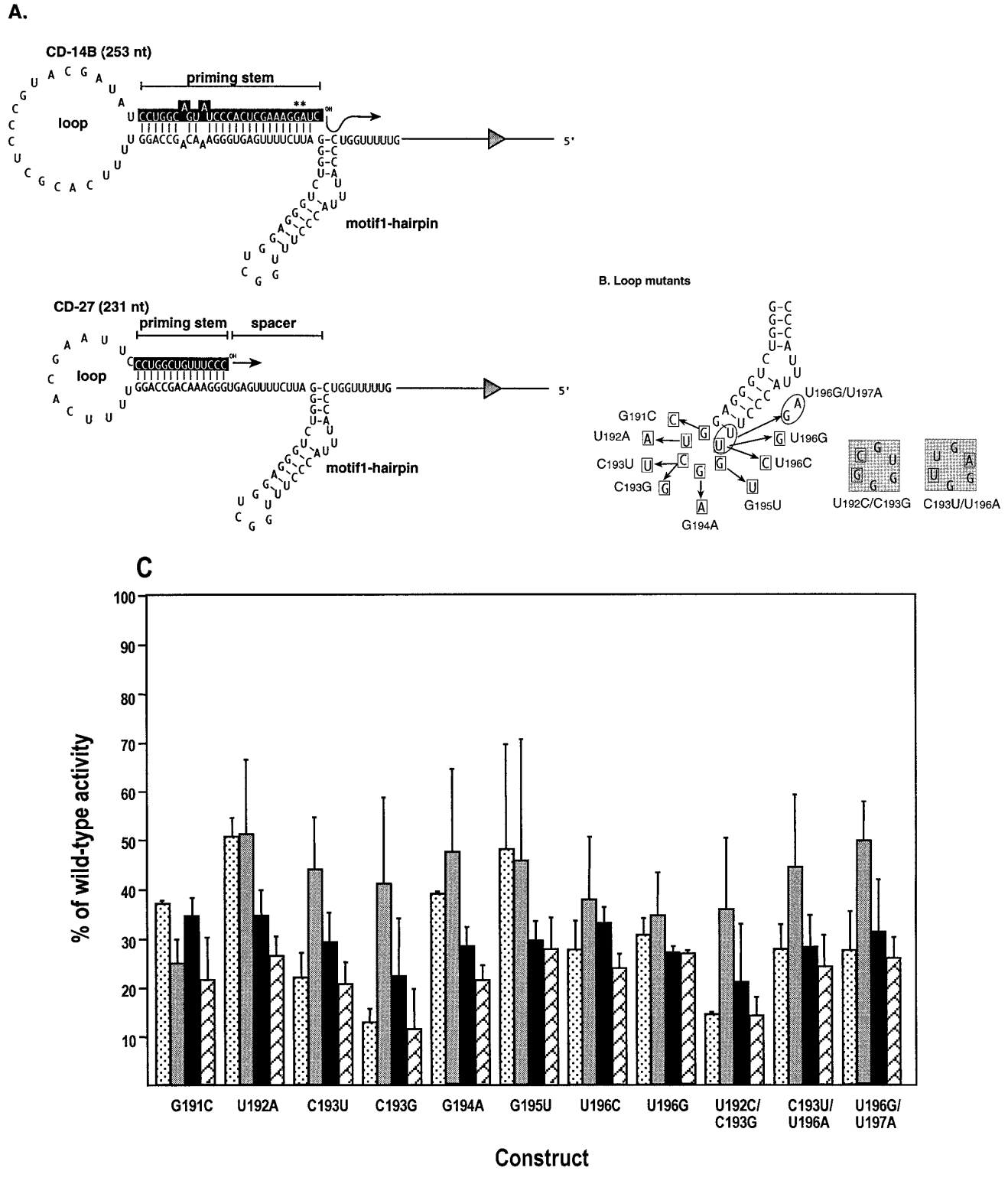

FIG. 3. The effect of mutations in the loop region of the motif1-hairpin on the level of 3′-terminal extension. (A) Top construct (CD-14B) contains 27 nts from sat-RNA D plus strand (boxed in black), extending from position −14 at the 3′ end, joined by a 5-base artificial sequence (GAUAU) to sat-RNA C minus-strand sequence that includes 43 nt 3′ of the motif1-hairpin, the motif1-hairpin, and the entire sat-RNA C sequence 5′ of the hairpin. Asterisks denote the positions of base alterations from wt sat-RNA D(+) (Fig. 1A) to generate a *Bam*HI site in the CD-14B construct. Bottom construct (CD-27), same as CD-14B, except that the sat-RNA D sequence terminates at the −27 position and two mismatches in the priming stem are mutated such that base-pairing can occur throughout the priming stem. Both constructs contain a promoter for positive-strand synthesis near the 5′ end as shown by triangles. (B) Single or multiple base changes were introduced into the motif1-hairpin sequence as shown. Mismatch-mutations are shown with single letters. The names of individual constructs are shown next to the mutations. Multiple mutations present in constructs U192C/C193G and C193U/U196A are shown separately with the loop sequences present in gray boxes. (C) Graphic representation of the relative amounts of 3′-terminal extension reactions obtained with mutants of (B). The effect on 3′-terminal extension by a particular mutation was tested in three separate constructs,

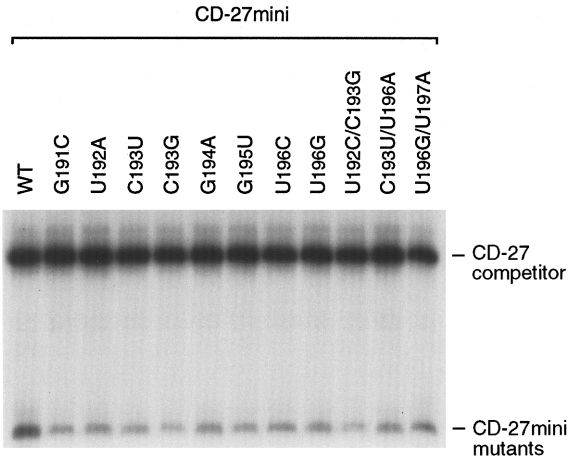

FIG. 4. 3′-terminal extension activity of loop mutants in a competition assay. A denaturing PAGE analysis showing the amount of 3′-terminal extension products synthesized by *in vitro* transcription with TCV RdRp using the shown motif1-hairpin loop mutants (Fig. 3B) in CD-27mini in the presence of a threefold molar excess of CD-27 (Fig. 3A).

level of 3′-terminal extension. Therefore, these data suggest that specific recognition of any of the nucleotides within the loop by the TCV RdRp is not absolutely required for 3′-terminal extension reaction. It is possible, however, that the RdRp recognizes several nucleotides in the motif1-hairpin. and therefore the simple mutagenesis strategy used here may result in only partial loss of RdRp binding and/or 3′-terminal extension activity.

To further analyze the role of loop mutations on 3′-terminal extension, we tested the 3′-terminal extension activity of loop mutants in a competition assay. Motif1-hairpin mutants that bind the RdRp inefficiently should be less active in 3′-terminal extension reactions under competitive conditions than in noncompetition assays because the RdRp and/or other components should be sequestered by the more competitive RNA construct with the wt motif1-hairpin. If a motif1-hairpin mutant binds the RdRp as efficiently as the wt, then the 3′-terminal extension activity of this particular mutant should be the same % of the wt level under competitive conditions as in noncompetition assays.

For the competition studies, CD-27 carrying the wt motif1-hairpin was used as a competitor in a threefold molar excess over the motif1-hairpin mutants in CD-27mini. The size difference between CD-27 and CD-27mini allowed for separate measurements of their 3′-terminal extension activity in the competition assay within a single gel (Fig. 4). The control experiment included wt CD-27 and wt CD-27mini, where the 3′-terminal extension activity of the latter construct represents the 100% value.

The 3′-terminal extension activity of loop mutants U192A, C193U, G194A, G195U, U196G, U192C/C193G, C193U/U196A, and U196G/U197A was less than 10% lower in the competition assay than in the noncompetition assay (Figs. 3B and 4), suggesting that these mutants may bind to the RdRp in the presence of an excess amount of wt motif1-hairpin as, or nearly as, efficiently as in its absence. Loop mutants G191C, C193G, and U196C had 3′-terminal extension activity that was 10–12% lower in the competition than in the noncompetition assay, suggesting a slightly lower affinity of these mutants for RdRp binding under competitive conditions. Nevertheless, each loop mutant showed higher than basal level of 3′-terminal extension in the competition assay, confirming the above findings that single and double mutations in the loop region can only partially inhibit 3′-terminal extension. Overall, this study supports a role for the loop sequences in recognition by the RdRp.

Mutations in the interior loop

Bulges within stem-loop structures are frequently recognized by proteins (Draper, 1995). The interior loop in the motif1-hairpin is asymmetrical containing one C (termed C bulge) opposite to three U residues (termed U bulge). This may cause a bend in the motif1-hairpin structure as schematically shown in Fig. 1. Deletion of the three U residues (construct ΔU3, Fig. 5A) was found to reduce 3′-terminal extension activity by 10-fold in CD-14B and eliminated *in vivo* recombination (Nagy *et al.,* 1998). This result indicated that the U bulge may play a specific role in recombination. However, the same U-bulge deletion has a much less detrimental effect on 3′-terminal extension when present in CD-27 and CD-27mini, with 63.2 and 67.5%, respectively, of the level of wt 3′-terminal extension (construct ΔU3, Fig. 5A). This suggests that the presence of a flexible spacer in CD-27 and CD-27mini can partially compensate for the adverse effect caused by the deletion of the U bulge when compared to CD-14B. However the competitiveness of ΔU3 was low (32.9% of wt level), suggesting that RdRp binding is much less efficient for the U-bulge deletion mutant than for the wt motif1-hairpin in the competition assay.

Mutagenesis of two or three U residues to either C or G nucleotides in the U bulge in CD-14B resulted in 30.6–52.8% of the wt 3′-terminal extension activity, while corresponding mutations in CD-27 and CD-27mini gave 56.2–76.4% and 74.0–89.9% level (constructs U203G/U204G, U203–205G,

CD-14B (strippled bars), CD-27 (gray bars), and CD-27mini (black bars). The 3′-terminal extension activity of each mutant was compared to the level obtained with the corresponding wt construct (100%). The fourth column (cross-hatched bar) shows the 3′-terminal extension activity of some of the CD-27mini series of constructs in the presence of a threefold excess of CD-27 (see also Fig. 4). The efficiency of 3′-terminal extension was analyzed by denaturing PAGE, followed by autoradiography and densitometry. The data were normalized based on the number of template-directed radioactive UTP incorporated. Standard error was calculated from two to three separate experiments.

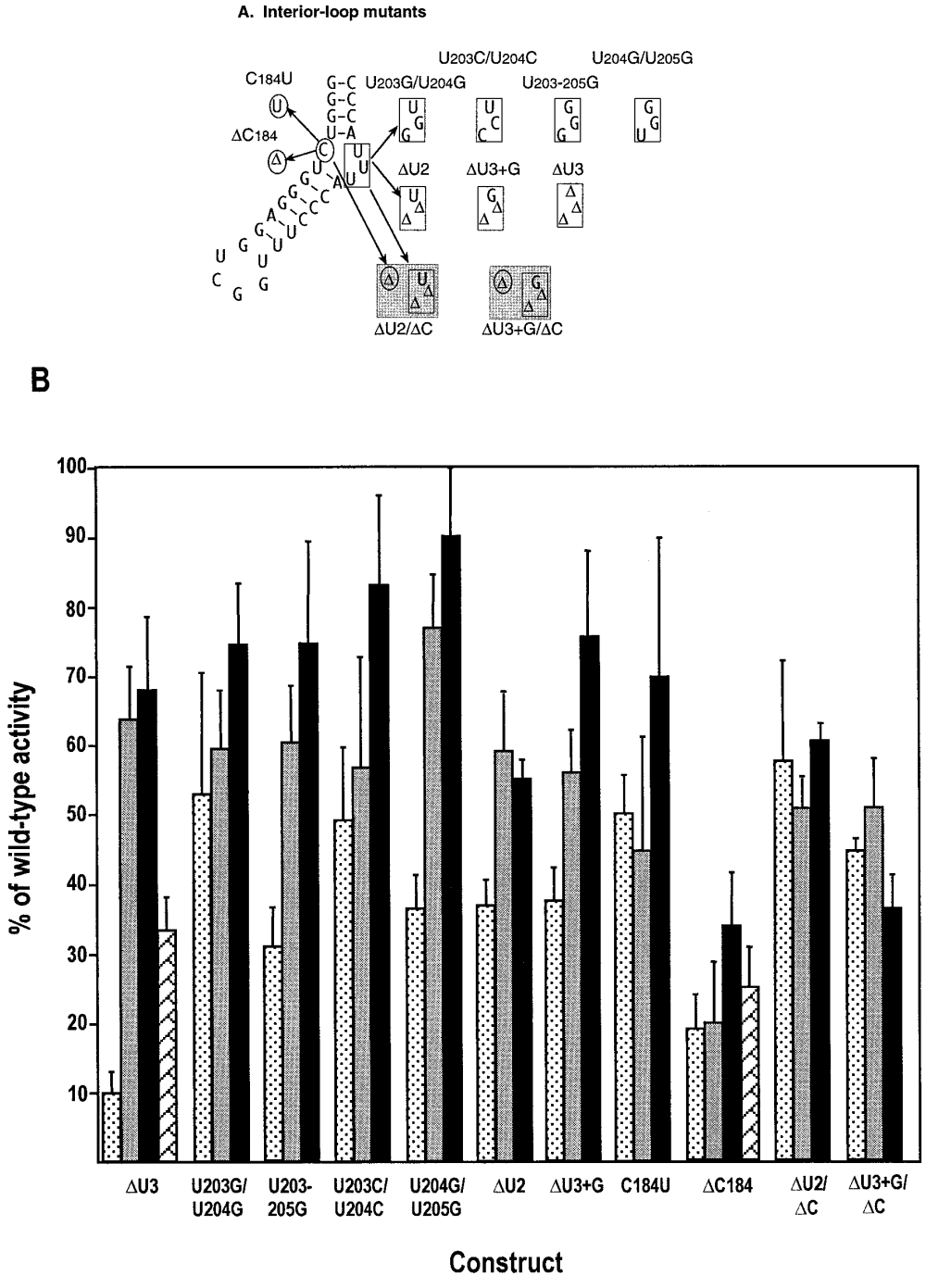

FIG. 5. The effect of mutations in the interior loop of the motif1-hairpin on the level of 3′-terminal extension. (A) Single or multiple base changes were introduced into the motif1-hairpin sequence as shown. Mismatch-mutations are shown with single letters, deletions are indicated by Δ. Multiple mutations present in a particular construct are shown separately. (B) Graphic representation of the relative amounts of 3′-terminal extension reactions obtained with mutants of (A). The data are shown as described in the legend to Fig. 3C.

U203C/U204C, U204G/U205G, Figs. 5A and 5B). These results suggest that the sequence of the U bulge only modestly affects recognition by the TCV RdRp.

To study the possible role of the structural distortion caused by the presence of the U bulge, deletion analysis was conducted. Deletion of two of the three U residues (constructs ΔU2) gave 3′-terminal extension activity of 36.7% of wt CD-14B, while the corresponding mutations had a less detrimental effect on 3′-terminal extension activity when present in CD-27 and CD-27mini with 58.6 and 54.5% of the level of wt activity (Fig. 5B). Deletion of two U residues in conjunction with a U-to-G mutation (construct ΔU3+G) should result in a motif1-hairpin with a C–G base pair in place of the asymmetrical interior loop, thus fusing the lower and upper stems into one large stem structure (Fig. 5A). Construct ΔU3+G gave

37.3% 3′-terminal extension activity of wt CD-14B, while the corresponding mutation in CD-27 and CD-27mini had 3′-terminal extension that was 56.1 and 75.5% of the level of wt activity (Fig. 5B). Overall, these data do not support a specific role for the U bulge in RdRp recognition. The higher inhibition of 3′-terminal extension activity for U-bulge deletion mutants in CD-14B than in CD-27 and CD-27mini may be explained by the less flexible positioning of the priming stem and the motif1-hairpin relative to one another in the CD-14B mutants.

Mutation of the single C residue in the C bulge (construct C184U) reduced 3′-terminal extension to 44.7–69.6% of wt (Fig. 5B), suggesting a modest amount of sequence-specific recognition of that C residue by the RdRp. Deleting the C-bulge (construct ΔC184) resulted in 18.5–33.4% 3′-terminal extension activity, indicating that RdRp interaction with the motif1-hairpin was more strongly affected. This was also supported by the low competitiveness of this mutant (25.0%, Fig. 5B). It is possible that deletion of the C-bulge changed the overall structure of the motif1-hairpin, resulting in reduced 3′-terminal extension activity.

Deletion of the C bulge had the most detrimental effect of the bulge mutations on 3′-terminal extension of all three constructs. However, when deletion of the C bulge was in conjunction with deletions in the opposite U-bulge region (see constructs ΔU2/ΔC and ΔU3+G/ΔC, Fig. 5A), the reduction of 3′-terminal extension activity was less pronounced (between 36.4 and 60.7%, Fig. 5B). This suggests that the C-bulge deletion can influence 3′-terminal extension mainly through structural effects on the entire motif1-hairpin.

Overall, deletion of the U or C bulge or their conversion into a G-C base pair are predicted to alter the conformation of motif1-hairpin around the interior loop region dramatically. Yet the extent of reduction in 3′-terminal extension was variable. This does not support specific RdRp recognition of either one or both bulge regions. Comparison of the 3′-terminal extension activity for all three sets of constructs revealed that most of the motif1-hairpin bulge mutations were less debilitating when present in CD-27 and CD-27mini than in CD-14B. It is possible that motif1-hairpins with altered structures in the interior loop region still can bind to the TCV RdRp, but the proper positioning of the 3′-OH of the primer stem is less efficient in the absence of the spacer.

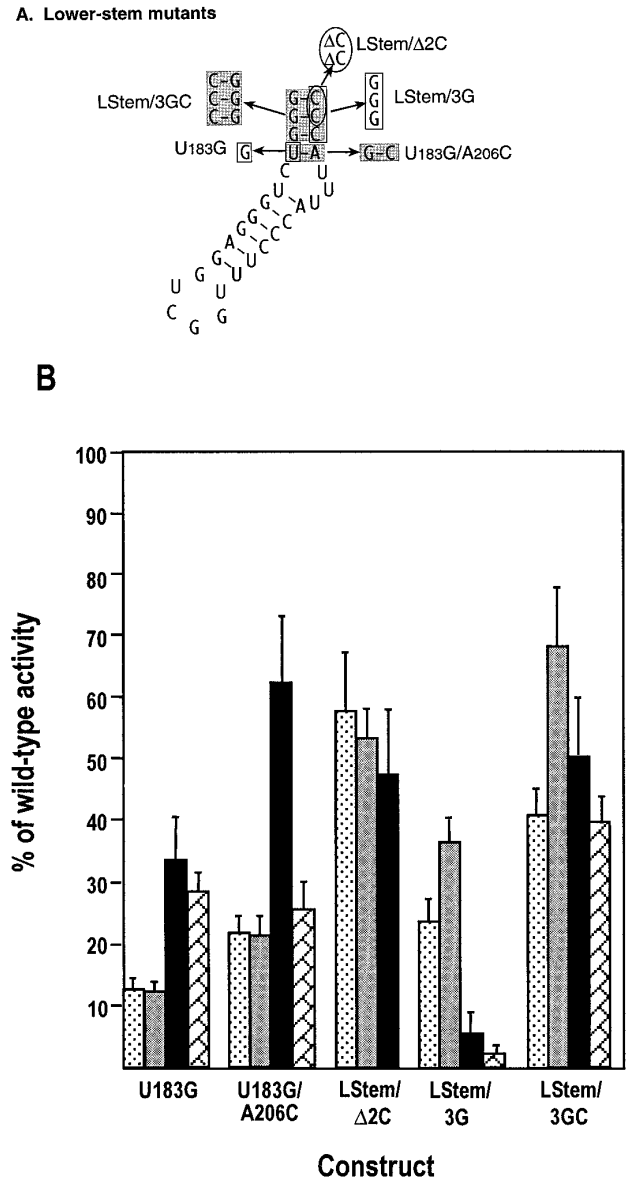

FIG. 6. The effect of mutations in the lower stem of the motif1-hairpin on the level of 3′-terminal extension. (A) Single or multiple base changes were introduced into the motif1-hairpin sequence as shown. Mismatch-mutations are shown with single letters, deletions are indicated by Δ, while compensatory mutations that preserved base pairing within the stem are shown with base-paired nucleotides in gray boxes. (B) Graphic representation of the relative amounts of 3′-terminal extension reactions obtained with mutants of (A). The data are shown as described in the legend to Fig. 3C.

Mutations in the lower stem

A single mutation that destabilized the lower stem of the motif1-hairpin in CD-14B and CD-27 (U183G, Fig. 6A) resulted in 3′-terminal extensions that were 12.3 and 12.4% of the level of the wt CD-14B and CD-27, respectively (Fig. 6B). U183G, when present in CD-27mini, resulted in 33.5% 3′-terminal extension when compared to CD-27mini with the wt motif1-hairpin. When U183G was combined with A206C (mutant U183G/A206C, Fig. 6A), resulting in a compensatory A–U to G–C base pair change, 3′-terminal extension was partially restored to 21.8, 21.5, and 62.2% in CD-14B, CD-27, and CD-27mini, respectively. The higher 3′-terminal extension activity of the CD-27mini mutants than that of CD-14B and CD-27 suggests that the mutated motif1-hairpin is more accessible for the RdRp in CD-27mini than in the other two constructs that contain lengthy 5′ sequences. Alternatively, the positive strand initiation promoter present in CD-14B and CD-27 constructs, but absent CD-27mini,

competes efficiently for RdRp binding against the mutated motif1-hairpin, thus reducing the level of 3′-terminal extension for CD-14B and CD-27 mutants. Comparing to the noncompetition assay, the 3′-terminal extension activity of mutant U183G in CD-27mini was reduced from 33.5 to 28.2% in the competition assay. The reduction was even more pronounced for construct U183G/A206C (from 62.2 to 25.4%), suggesting a reduced affinity for RdRp binding under competitive conditions. In addition, these data demonstrate that the A–U base pair in the lower stem is favored over a G–A mismatch or a G–C base pair.

Deletion of two C residues decreased 3′-terminal extension to 47.6 to 57.9% (mutant LStem/Δ2C, Fig. 6A). Mutating the three C residues to three G residues destabilized the lower stem of the motif1-hairpin in LStem/3G and resulted in 3′-terminal extension of 23.5 and 36.5% for CD-14B and CD-27, while only 5.9% of 3′-terminal extension activity remained when the alterations were incorporated into CD-27mini. In addition, LStem/3G in CD-27mini showed a basal level of 3′-terminal extension activity in the competition assays, indicating that the motif1-hairpin was nonfunctional. In contrast, LStem/3G in CD-14B and CD-27 resulted in ~10-fold higher (23.5 and 36.6% for CD-14B and CD-27) than basal level of 3′-terminal extension activity, suggesting that interaction between the mutated lower stem and some 5′ flanking sequences may partly restore the motif1-hairpin function.

Restoring the three G–C base pairs in the lower stem of the motif1-hairpin by compensatory mutations (construct LStem/3GC, Fig. 6A) increased the level of 3′-terminal extension to 41.0–68.8%. In the competition assay, LStem/3G and LStem/3GC showed 2.2 and 39.5% activity, respectively. Taken together, these results suggest that the three C–G and one A–U base pairs in the lower stem are critical for high 3′-terminal extension activity. Changing the three C–G base pairs to G–C base pairs reduces 3′-terminal extension, although not as much as when the lower stem is destabilized by three G–G mismatches. If the three C–G base pairs have a structure similar to three G–C base pairs, then the reduction in 3′-terminal extension activity for construct LStem/3GC as compared to the wt suggests that the primary sequence of the lower stem also plays a role in 3′-terminal extension.

Mutations in the upper stem

A single mismatch mutation (construct U185G, Fig. 7A) in the upper stem resulted in 6.8, 34.0, and 48.5% of wt 3′-terminal extension activity when present in CD-14B, CD-27, and CD-27mini, respectively (Fig. 7B). When U185G was combined with A202C, resulting in a compensatory A–U to G–C base pair change (construct U185G/A202C, Fig. 7A), 3′-terminal extension activity was increased to 24.4, 56.7, and 73.8% of wt activity (Fig. 7B). In the competition assay, mutants U185G and U185G/A202C gave 33.3 and 69.2% 3′-terminal extension activity. This suggests that the U–A base pair is favored over a G–C base pair or mismatch nucleotides next to the interior loop region. The higher activity of CD-27 and CD-27mini constructs than the corresponding CD-14B constructs indicate that this position is less important for RdRp binding, but rather it may influence the positioning of the motif1-hairpin and the priming stem relative to one another.

Another mutation that destabilized the upper stem (construct A189U, Fig. 7A) gave 3′-terminal extension activity of 22.9–45.0%. Exchanging the three G–C base pairs with three C–G base pairs (construct UStem/3GC) reduced 3′-terminal extension to 25.4% of wt CD-14B, while the analogous mutations in CD-27 and CD-27mini resulted in 69.4 and 52.0% 3′-terminal extension activity. The higher level of 3′-terminal extension activity for CD-27 and CD-27mini than that of CD-14B suggests that, similar to the neigbouring A–U base pair located next to the interior loop region (see above), this region is important in positioning of the motif1-hairpin and the priming stem relative to one another rather than in binding to the RdRp.

More extensive mutagenesis that weakened the stability of the upper stem in construct UStem32 reduced 3′-terminal extension activity to 8.3–20.9% (Fig. 7B). Similar disruptive mutagenesis of the upper stem in UStem43 and UStem48 decreased 3′-terminal extension to 12.2–24.3%. These constructs also competed poorly in the competition assays (6.2–10.5% activity). Construct UStem44, which contained a weak stem structure with two consecutive stable base pairs (G–C and C–G base pairs), supported 3′-terminal extension at 18.8, 20.2, and 42.9% of the wt level for CD-14B, CD-27, and CD-27mini, respectively (Fig. 7B). UStem44 was more competitive than the above UStem mutants, suggesting that two consecutive stable base pairs are important in 3′-terminal extension. Taken together, none of the mutations in the upper stem decreased 3′-terminal extension to the basal level, indicating the lack of specific sequence requirements for RdRp binding. A strong preference for the presence of stable base pairs was observed in this region, although replacing a A–U base pair with G–C base pair, which resulted in four consecutive G–C pairs, also decreased 3′-terminal extension activity. Some of the mutants supported a role of the upper stem in positioning of the motif1-hairpin and the priming stem relative to one another rather than in binding to the RdRp.

This study unexpectedly reveals the complex nature of the 3′-terminal extension reaction in TCV, since similar motif1-hairpin mutations when present in different constructs gave frequently very different 3′-terminal extension activity. For example, comparison of the 3′-terminal extension activity for all three series of constructs revealed that most of the mutations were less debilitating when present in the motif1-hairpins of CD-27 and CD-

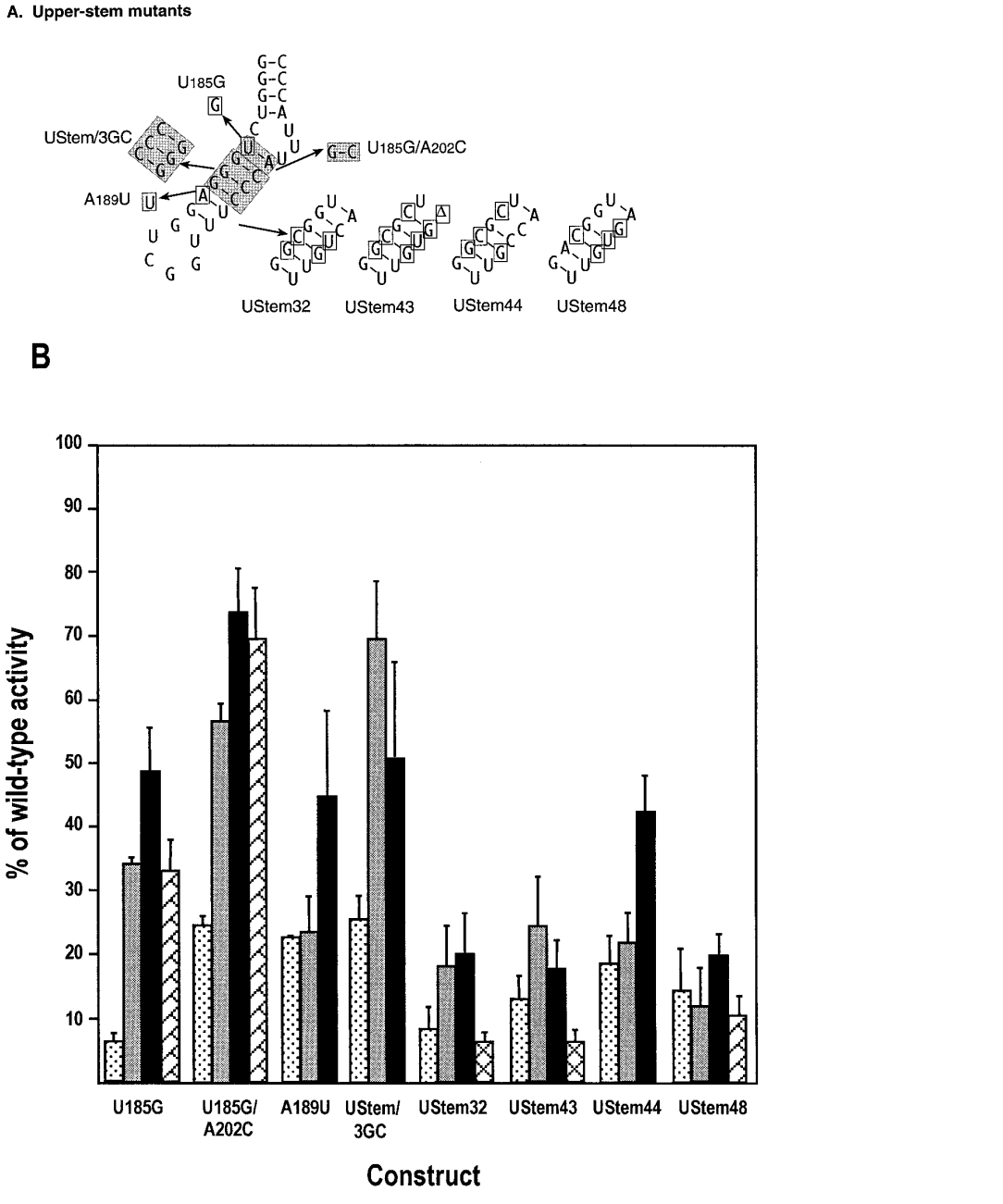

FIG. 7. The effect of mutations in the upper stem of the motif1-hairpin on the level of 3′-terminal extension. (A) Single or multiple base changes were introduced into the motif1-hairpin sequence as shown. Mismatch-mutations are shown with single letters, deletions are indicated by Δ, while compensatory mutations that preserved base pairing within the stem are shown with base-paired nucleotides in gray boxes. Multiple mutations in UStem32, UStem43, UStem44, and UStem48 are shown separately. (B) Graphic representation of the relative amounts of 3′-terminal extension reactions obtained with mutants of (A). The data are shown as described in the legend to Fig. 3C.

27mini than in CD-14B. Another general trend was that the highest 3′-terminal extension activity was observed for the CD-27mini constructs, suggesting that the motif1-hairpin and/or the priming stem is more accessible in the absence of extensive 5′ sequences that include a positive-strand initiation (transcriptional) promoter. Competition experiments between the mutated and wt motif1-hairpin constructs demonstrated that most of the mutants supported 3′-terminal extension only at a slightly reduced level in the competition assays as compared to the noncompetition assays. Based on these observations, we suggest that the role of the motif1-hairpin in 3′-terminal extension is complex and can be influenced by flanking sequences. We propose that in addition to recruiting the RdRp, the motif1-hairpin may play a role in positioning the priming stem (or the 3′-OH group of the 3′-terminal nucleotide) "properly" to the catalytic center of the RdRp. Some motif1-hairpin mutations may change how the RdRp binds to the hairpin (i.e., the location of catalytic center relative to the priming stem may be

altered for some mutants). If there is a flexible spacer element between the priming stem and the motif1-hairpin, this spacer may increase the efficiency of 3′-terminal extension by allowing the proper presentation of the priming stem for the bound RdRp before initiation of RNA synthesis. This may result in an increased 3′-terminal extension activity for CD-27 and CD-27mini mutants. In contrast, motif1-hairpin mutations may inhibit 3′-terminal extension to a larger extent for CD-14B since the spacer region is part of the priming-stem (i.e., base-paired in CD-14B) and therefore, it may disfavor the proper presentation of the priming stem for the bound RdRp. Thus according to this model, both RdRp binding and proper positioning of the 3′ end of the primer stem are important for 3′-terminal extension. This would explain why CD-27 and CD-27mini with a single-stranded spacer can retain more activity than CD-14B with no spacer for several hairpin mutants.

None of the motif1-hairpin mutations tested showed basal level of 3′-terminal extension with all three sets of constructs. Therefore, this study suggests that none of the nucleotides within the motif1-hairpin is absolutely required for 3′-terminal extension. Overall, the results of the mutagenesis and competition experiments suggest that the TCV RdRp recognizes the secondary and/or tertiary structure of the motif1-hairpin. In addition, the sequence of the motif1-hairpin possibly plays a role through either directly influencing RdRp binding or indirectly by altering the secondary and/or tertiary structure of the motif1-hairpin. Therefore recognition of the motif1-hairpin by the TCV RdRp may be similar to the recognition of subgenomic promoters on the TCV minus strands (Wang and Simon, 1997) and the negative strand initiation promoter on sat-RNA C (Song and Simon, 1995; Stupina and Simon, 1997; Carpenter and Simon, 1998). These promoter sequences contain hairpin structures that are required for complementary RNA synthesis. In addition to the hairpin structures, TCV RdRp also recognizes short primary sequences with multiple consecutive C residues followed by multiple consecutive purines present on the negative-stranded sat-RNA C (Guan *et al.,* 1997). Direct RdRp-binding experiments will be useful to elucidate the mechanism of motif1-hairpin recognition.

In summary, results presented in this and previous papers (Nagy *et al.,* 1998) suggest that the TCV RdRp recognizes the secondary and/or tertiary structure of the motif1-hairpin, while individual nucleotides play a less important role. Recognition of the motif1-hairpin by the RdRp may be important in recruiting the RdRp, either complexed with the nascent strand or in its "free" form during the template switching events. The motif1-hairpin may also play a role in proper presentation of the 3′-terminal nucleotide, which is part of the priming stem, to the catalytic center of the RdRp.

In addition to its role in RNA recombination, the motif1-hairpin has a *cis*-acting function in replication of sat-RNA C (P. D. Nagy, J. Pogany, and A. E. Simon, unpublished data). It is possible that *cis*-acting elements or sequences that resemble *cis*-acting elements may play a role in RNA recombination in other viral systems as well. For example, some of the junction sites in flock house virus, an animal nodavirus, resemble a replication origin located at the extreme 3′ terminus of RNA2 (Ball, 1997). The similarity of the junction site sequences to the 3′ replication origin suggests that internal sequences may guide the polymerase during template switching (Ball, 1997). In addition, subgenomic RNA promoters or related sequences are frequently found as recombination sites in BMV (Allison *et al.* 1990), Sindbis virus (Weiss and Schlesinger, 1991), tobacco mosaic virus (Beck and Dawson, 1990), citrus tristeza virus (Bar-Joseph *et al.,* 1997), and TCV (C. D. Carpenter and A. E. Simon, unpublished results). Many crossover events in BMV (Nagy and Bujarski, 1992; Rao and Hall, 1993), Sindbis virus (Hajjou *et al.,* 1996), tobraviruses (Goulden *et al.,* 1991), cucumoviruses (Fernandez-Cuartero *et al.,* 1994), alfalfa mosaic virus (Huisman *et al.,* 1989), and barley stripe mosaic virus (Edwards *et al.,* 1992) are located within 3′ or 5′ terminal promoter sequences. These terminal or internal *cis*-acting sequences may have played a role in recombination events by recruiting the RdRp/nascent strand complex.

MATERIALS AND METHODS

RNA template construction

RNA templates were obtained by *in vitro* transcription with T7 RNA polymerase using either PCR-amplified DNA templates (constructs CD-13mini, CD-27mini, and CD-27 and their derivatives) or purified and *Bam*HI-linearized plasmid DNA (construct CD-14B and its derivatives) (Song and Simon, 1994; Nagy *et al.,* 1997). After phenol/chlorophorm extraction, unincorporated nucleotides were removed by repeated ammonium-acetate/isopropanol precipitation (Song and Simon, 1994; Nagy *et al.,* 1997). The obtained RNA transcripts were dissolved in sterile water, and their amount and size were measured by a UV spectrophotometer and 5% polyacrylamide/8 M urea gel (denaturing PAGE) analysis (Song and Simon, 1994; Nagy *et al.,* 1997).

Constructs CD-13mini, CD-27mini, CD-27, and CD-14B have been generated previously (Nagy *et al.,* 1998). The following derivatives of CD-14B with mutations in the motif1-hairpin were also available: U183G, U183G/A206C, LStem/Δ2C, LStem/3G, LStem/3GC, U185G, U185G/A202C, A189U, UStem/3GC, ΔU3, G191C, U192A, C193U, G194A, G195U, and U196C (Nagy *et al.,* 1998).

Constructs U203G/U204G, U203–205G, U203C/U204C, U204G/U205G are derivatives of CD-14B and were constructed by PCR with primers hairpin-satD [5′-GGG(A/T)-(A/T)CCTTTCGAGTGGGATACTGCCAGGATATCGTACGG-GAGCGTG-3′], and bulgemod [5′-GGACGGGGCCCA(G/T/C) (G/T/C) (G/T/C)ACCCTTTGGCTG-3′], while ΔC184 was obtained with primers hairpin-satD and har-dC (5′-TTTTGGGCCCATTTACCCTTTGGCTGGAGGGTTGGG-3′) on CD-14B template. Constructs C193G, U192C/C193G,

C193U/U196A, U196G/U197A, and U196G were obtained by PCR with primers hairpin-satD and loop-mod [5′-GCACGGGGCCCATTTACCCT(A/T/C)(G/A/T)GG(C/T)TGGAGGGTCTGG-3′], while C184U was generated with primers hairpin-satD and C-bulgemod [5′-GCACGGGGCCCATTTACCCTTTGGCTG(A/G)AGGGT(A/T/C)TGGGA-3′] on CD-14B template. Constructs UStem32, UStem43, UStem44, and UStem48 were generated by PCR with primers hairpin-satD and stem-mod2 [5′-GCACGGGGCCCATTTA(G/C)(C/T)GTTTGGCTGG(A/G)C(A/G)(G/C)TCTGG-3′], while constructs ΔU2 and ΔU3+G were obtained by PCR with primers hairpin-satD and DUU [5′-GGACGGGGCCCA(G/T)ACCCTTTGG-3′] on CD-14B template. Constructs ΔU2/ΔC, ΔU3+G/ΔC were obtained using primers hairpin-satD and DUU on ΔC templates. All the above PCR products were digested with *Apa*I and *Eco*RV and cloned into the similarly treated CD-14B. The appropriate clones were selected by sequencing.

All the above CD-14B derivatives were used separately to generate CD-27 and CD-27mini series of constructs. CD-27 derivatives were obtained with two sequential rounds of PCR, first using primers hairpin-1 [5′-GGG(A/T)(A/T)(A/T)(C/T)AGCCAGGGAATTCGTGAAAACCTGGCTG-3′] and T7C3′ (5′-GTAATACGACTCACTATAGGGCAGGCCCCCCG-3′) and the corresponding CD-14B templates. This was followed by a second round of PCR with primers har1/0 (5′-GGGAAACAGCCAGGGAATTCGTGA-3′) and T7C3′. CD-27mini series of constructs were also obtained by PCR with primers har1/0 and T7motif1 (5′-GTAATACGACTCACTATAGGGCTGCCGCCGTTTTTGG-3′) using the corresponding CD-27 derivatives as template. Constructs CD-27mini/random2 and CD-27mini/random6 were obtained with primers hairpin-1 and T7C3′ using Selex/28–2 and Selex/28–6 templates (generous gift of Ben deRuyter), followed by a second round of PCR with primers har1/0 and T7motif1. Constructs CD-13mini/random2 and CD-13mini/random6 were obtained with primers CD-13 (5′-GGACTCTTTCGAGTGGGATACTGCCAGGGAATTCGTGA-3′) and T7motif1, using CD-27mini/random2 and CD-27mini/random6 templates. The PCR products were purified and used for RNA transcription.

3′-terminal extension product analysis

Preparation of template-dependent RdRp from TCV-infected turnip plants, *in vitro* 3′-terminal extension reactions (similar to transcription reactions, but using different RNA templates), and product analysis was carried out as previously described (Song and Simon, 1994; Nagy *et al.,* 1997; 1998) using a total RdRp reaction mixture of 20 μl that contained 3 μg of template RNA. For the competition studies, 6 μg of CD-27 and 1 μg of CD-27mini derivatives were used in a 20 μl RdRp reaction mixture.

After phenol/chlorophorm extraction and ammonium-acetate/isopropanol precipitation, the products were analyzed on a 20-cm-long denaturing 5% PAGE/8 M urea gel, followed by autoradiography and densitometry (Nagy *et al.,* 1997). The data were normalized based on the number of template-directed radioactive UTP incorporated into the 3′-terminal extension products and the molar amount of the template RNA in the RdRp reaction. For some experiments, gels were stained with ethidium bromide, photographed and dried, followed by analysis with a phosphorimager as described (Nagy *et al.,* 1997).

ACKNOWLEDGMENTS

We thank Dr. Judit Pogany for critical reading of the manuscript. This work was supported by National Science Foundation Grants MCB-9630191 and MCB-9728277 to A.E.S.

REFERENCES

Allison, R. F., Thompson, G., and Ahlquist, P. (1990). Regeneration of a functional RNA virus genome by recombination between deletion mutants and requirement for cowpea chlorotic mottle virus 3a and coat genes for systemic infection. *Proc. Natl. Acad. Sci. USA* 87, 1820–1824.

Ball, L. A. (1997). Nodavirus RNA recombination. *Semin. Virol*. 8, 95–100.

Bar-Joseph, M., Yang, G., Gafny, R., and Mawassi, M. (1997). Subgenomic RNAs: The possible building blocks for modular recombination of *Closteroviridae* genomes. *Semin. Virol*. 8, 113–119.

Beck, D. L., and Dawson, W. O. (1990). Deletion of repeated sequences from tobacco mosaic virus mutants with two coat protein genes. *Virology* 177, 462–469.

Buck, K. W. (1996). Comparison of the replication of positive-stranded RNA viruses of plants and animals. *Adv. Virus Res.* 47, 159–251.

Cascone, P. J., Carpenter, C. D., Li, X. H., and Simon, A. E. (1990). Recombination between satellite RNAs of turnip crinkle virus. *EMBO J.* 9, 1709–1715.

Cascone, P. J., Haydar, T. F., and Simon, A. E. (1993). Sequences and structures required for recombination between virus-associated RNAs. *Science* 260, 801–805.

Chetverin, A. B., Chetverina, H. V., Demidenko, A. A., and Ugarov, V. I. (1997). Nonhomologous RNA recombination in a cell-free system: Evidence for a transesterification mechanism guided by the secondary structure. *Cell* 88, 503–513.

Dolja, V. V., and Carrington, J. C. (1992). Evolution of positive-strand RNA viruses. *Semin. Virol.* 3, 315–326.

Draper, D. E. (1995). Protein–RNA recognition. *Annu. Rev. Biochem.* 64, 593–620.

Edwards, M. C., Petty, I. T. D., and Jackson, A. O. (1992). RNA recombination in the genome of barley stripe mosaic virus. *Virology* 189, 389–392.

Fernandez-Cuartero, B., Burgyan, J., Aranda, M. A., Salanki, K., Moriones, E., and Garcia-Arenal, F. (1994). Increase in the relative fitness of a plant virus RNA associated with its recombinant nature. *Virology* 203, 373–377.

Goulden, M. G., Lomonossoff, G. P., Wood, K. R., and Davies, J. W. (1991). A model for the generation of tobacco rattle virus (TRV) anomalous isolates: Pea early browning virus RNA2 acquires TRV sequences from both RNA-1 and RNA-2. *J. Gen. Virol.* 72, 1751–1754.

Guan, H., Song, C., and Simon, A. E. (1997). RNA promoters located on (−)-strands of a subviral RNA associated with turnip crinkle virus. *RNA* 3, 1401–1412.

Hajjou, M., Hill, K. R., Subramaniam, S. V., Hu, J. Y., and Raju, R. (1996). Nonhomologous RNA-RNA recombination events at the 3′ nontranslated region of the Sindbis virus genome: Hot spots and utilization of nonviral sequences. *J. Virol*. 70, 5153–5164.

Huisman, M. J., Cornelissen, B. J. C., Groenendijk, C. F. M., Bol, J. F., and Van Vloten-Doting, L. (1989). Alfalfa mosaic virus temperature-sensitive mutants V. The nucleotide sequence of TBTS 7 RNA 3 shows

limited nucleotide changes and evidence for heterologous recombination. *Virology* 171, 409–416.

Jarvis, T. C., and Kirkegaard, K. (1991). The polymerase in its labyrinth: Mechanisms and implications of RNA recombination. *Trends Genet.* 7, 186–191.

King, A. M. Q. (1988). Genetic recombination in positive strand RNA viruses. *In* "RNA Genetics," (E. Domingo, J. J. Holland, and P. Ahlquist, Eds.), Vol II, pp. 149–185. CRC Press, Boca Raton, FL.

Lai, M. C. M. (1992). RNA recombination in animal and plant viruses. *Microbiol. Rev.* 56, 61–79.

Nagy, P. D., and Bujarski, J. J. (1992). Genetic recombination in brome mosaic virus: Effect of sequence and replication of RNA on accumulation of recombinants. *J. Virol*. 66, 6824–6828.

Nagy, P. D., and Bujarski, J. J. (1993). Targeting the site of RNA-RNA recombination in brome mosaic virus with antisense sequences. *Proc. Natl. Acad. Sci. USA* 90, 6390–6394.

Nagy, P. D., and Bujarski, J. J. (1995). Efficient system of homologous RNA recombination in brome mosaic virus: Sequence and structure requirements and accuracy of crossovers. *J. Virol.* 69, 131–140.

Nagy, P. D., and Bujarski, J. J. (1996). Homologous RNA recombination in brome mosaic virus: AU-rich sequences decrease the accuracy of crossovers. *J. Virol.* 70, 415–426.

Nagy, P. D., and Bujarski, J. J. (1997). Engineering of homologous recombination hotspots with AU-rich sequences in brome mosaic virus: AU-rich sequences decrease the accuracy of crossovers. *J. Virol.* 71, 3799–3810.

Nagy, P. D., Carpenter, C. D., and Simon, A. E. (1997). A novel 3′-end repair mechanism in an RNA virus. *Proc. Natl. Acad. Sci. USA* 94, 1113–1118.

Nagy, P. D., and Simon, A. E. (1997). New insights into the mechanisms of RNA recombination. *Virology* 235, 1–9.

Nagy, P. D., Zhang, C., and Simon, A. E. (1998). Dissecting RNA recombination *in vitro*: Role of RNA sequences and the viral replicase. *EMBO J.* 17, 2392–2403.

Rao, A. L. N., and Hall, T. C. (1993). Recombination and polymerase error facilitate restoration of infectivity in brome mosaic virus. *J. Virol.* 67, 969–979.

Simon, A. E., and Bujarski, J. J. (1994). RNA-RNA recombination and evolution in virus infected plants. *Annu. Rev. Phythopathol.* 32, 337–362.

Simon, A. E., and Howell, S. H. (1986). The virulent satellite RNA of turnip crinkle virus has a major domain homologous to the 3′ end of the helper virus genome. *EMBO J.* 5, 3423–3428.

Simon, A. E., and Nagy, P. D. (1996). RNA recombination in turnip crinkle virus: Its role in formation of chimeric RNAs, multimers, and in 3′-end repair. *Semin. Virol.* 7, 373–379.

Song, C., and Simon, A. E. (1994). RNA-dependent RNA polymerase from plants infected with turnip crinkle virus can transcribe (+) and (−)-strands of virus-associated RNAs. *Proc. Natl. Acad. Sci. USA* 91, 8792–8796.

Song, C., and Simon, A. E. (1995). Requirement of a 3′-terminal stem-loop in *in vitro* transcription by an RNA-dependent RNA polymerase. *J. Mol. Biol.* 254, 6–14.

Strauss, J. H., and Strauss, E. G. (1988). Evolution of RNA viruses. *Annu. Rev. Microbiol.* 42, 657–683.

Stupina, V., and Simon, A. E. (1997). Analysis *in vivo* of turnip crinkle virus satellite RNA C variants with mutations in the 3′-terminal Minus-strand promoter. *Virology* 238, 470–477.

Wang, J., and Simon, A. E. (1997). Analysis of the two subgenomic RNA promoters for turnip crinkle virus *in vivo* and *in vitro*. *Virology* 232, 174–186.

Weiss, B. G., and Schlesinger, S. (1991). Recombination between Sindbis virus RNAs. *J. Virol.* 65, 4017–4025.

White, K. A., and Morris, T. J. (1995). RNA determinants of junction site selection in RNA virus recombinants and defective interfering RNAs. *RNA* 1, 1029–1040.

Zimmern, D. (1988). Evolution of RNA viruses. *In* "RNA Genetics" (J. J. Holland, E. Domingo, and P. Ahlquist, Eds.), Vol. II, pp. 211–240, CRC Press, Boca Raton, FL.